

Semi-Analytical Method Based on Magnetic Equivalent Circuit for Synchronous Permanent-Magnet Machines in EV and HEV Applications

S.A. Randi^a, R. Benlamine^a, F. Dubas^b, and C. Espanet^b

^a Renault SAS, 78288 Guyancourt, France

^b FEMTO-ST Institute, UFC, ENERGIE Department, UMR 6174 CNRS, 90010 Belfort, France

Abstract

Concentrated Winding Permanent-Magnet (PM) Synchronous Machines (CWPSM) are more and more used to drive electromechanical systems working in variable speed mode, such as Electric Vehicle (EV) and Hybrid Electric Vehicle (HEV) applications. In order to design and optimize these machines, the authors propose a semi-analytical method based on magnetic equivalent circuit (MEC). The studied structure, 12-slots/8-poles CWPSM, is an internal rotor topology with surface mounted PMs having radial magnetization. We compare the results obtained with finite-element analysis (FEA) with those given by the MEC. In this paper both precision and time computation are evaluated in order to analyse the possible implementation of the model in an optimal design tool.

Keywords: Concentrated winding, Permanent-magnet, Synchronous machines, Magnetic equivalent circuit, Finite-element analysis.

Nomenclature

H_s	the magnetic field calculated by Marrocco interpolation
B_s	the flux density
b_s	reduced value of the flux density B_s ($b_s = \frac{B_s}{1T}$)
μ_0	the vacuum permeability
K_i	the Marrocco interpolation coefficients ($i=1, \dots, 4$)
\mathfrak{R}_r	radial reluctances
\mathfrak{R}_θ	tangential reluctances
\mathfrak{R}	the reluctances matrix
S	the loop matrix
F	the sources vector
Φ	the loop fluxes vector
φ	the reluctance fluxes vector
S_R	the reluctance surface vector
F_{pm}	the magneto-motive force provided by PM
F_l	the magneto-motive force provided by a coil
h_a	the thickness of the PM
n_t	the number of turns per coil
I_s	the phase current
N_L	the loops number in the reluctance network

N_R the reluctances number in the reluctance network
--

1. Introduction

If symbols are used extensively, a nomenclature list arranged alphabetically, with Greek, subscript and superscript symbols listed separately, should be provided. Put a nomenclature above the main text if necessary, in a box with the same font size as the rest of the paper. Otherwise all symbols should be identified when first used in the text. The unit of the nomenclatures should be clarified following the description text. Authors are expected to use the SI system of units. Use Mathtype software to edit nomenclatures with Greek characters. Here introduce the paper, and the paragraphs continue from here and are only separated by headings, subheadings, images and formulae. The section headings are arranged by numbers, bold and 12 pt. Here follows further instructions for authors.

The design of electric machines for variable speed applications such as EV and HEV is a difficult problem. Indeed when a designer has to define a new electric machine for a given application, he has to solve the problem of sizing parameters (i.e., the nominal and maximum torque, the rated and maximal speed, the nominal and maximal current...). In classical industrial application when the electric machine has only a few operating points in the torque speed plane, the sizing torque and base speed can be found easily. In EV and HEV, there is a large dispersion of operating points in the torque speed plane [5]. Therefore to find the best solution designers must evaluate a lot of machines characterized by different sizing torques and base speeds. Furthermore when the sizing torque and the base speed are known, designer must answer to a lot of questions: which machine technology, what is the topology (e.g., the number of slots, the number of poles), the winding (e.g., distributed, concentrated...), the major geometric dimensions, etc. Due to the complexity of the sizing, it is clear that that optimization can help the designer to find a new electric machine for EV and HEV. Beside, the size of the optimization problem is related to the number of input parameters (i.e., the sizing parameters, the technology parameters, the topology parameters, the geometric parameters...); finally we must often evaluate hundred thousands of solutions to find the best one. To evaluate the criteria, optimization process must be linked to a model of the electric machine. There is a lot of modelling approach in electric machine, depending on the level of precision and the computation time. Regarding the concordance with measurement, the FEA seems today the best one, if we want to consider complex geometry and magnetic saturation. Unfortunately, this approach cannot be coupled easily with an optimization procedure, because the evaluation of one solution with FEA is quite time consuming (i.e., it can take up to few minutes or even hours).

In this paper, we present a semi-analytical modelling approach for the electric machines based on the MEC [6]-[8]. The electric Machine used to present the modelling methodology is a CWPMSM [8]. Those machines are more and more used in automotive applications because they enable a great reduction of copper weight (thus a great reduction of axial length, copper losses and cost) and they offer the advantage of a fully automatized winding process. In section 2.1, we give a brief description of the machine geometry. Then, we explain how the saturation effect is taken into account in section 2.2. In section 2.3, we present the MEC dealing with radial and tangential reluctances The discretization and resolution method are presented in section 2.4. In section 3, we discuss the precision and computation time of the MEC and the section 4 deals with the comparison between the MEC and FEA: we show that the computation time can be divided by 10 with using MEC, without a strong information loss.

2. Semi-Analytical Modelling via MEC

2.1. Electrical Machine Description and Assumptions

The machine considered in this work is a 12-slots/8-poles CWPMSM. This studied structure is an internal rotor topology with surface mounted PMs having radial magnetization. To reduce the computation time, the study of the machine can be carried out over one electric period under only 3-slots/2-poles, as shown in Figure 1. The electrical steel M330-35A of Arcelor Mittal is used for this machine. The main parameters of the 12-slots/8-poles CWPMSM are reported in Table 1. The concentrated winding configuration is presented in Figure 6.

2.2. Saturation effect

Follow this order when typing manuscripts: Title, Authors, Affiliations, Abstract, Keywords, Main text (including figures and tables), Acknowledgements, References, and Appendix. Collate acknowledgements in a separate section at the end of the article and do not include them on the title page, as a footnote to the title or otherwise.

To introduce the saturation effect in the model, the Marrocco's function is used [1]-[3]. Four interpolation coefficients (i.e. $k_1 \sim k_4$) are used in the formula. They are calculated according to the vendor data and with using the least squares method. The Figure 2 shows that the used coefficients give a good agreement between the B(H) curve given by the manufacturer and the interpolated function given by the Marrocco's function and described herein by

$$H_S^i(B_S^i) = \frac{B_S^i}{\mu_0} \cdot \left[\frac{b_S^{2k_1} \cdot (k_4 - k_1)}{b_S^{2k_1} + k_1} + k_2 \right] \quad (1)$$

The relative permeability function is presented by

$$\mu_r^i(B_S^i) = \frac{B_S^i}{\mu_0 \cdot H_S^i(B_S^i)} \quad (2)$$

2.3. Reluctances computation

Each region i of the machine, having the same magnetic permeability, can be described by two tangential and two radial reluctances, with a mid-point, as shown in Figure 3. Then, the MEC of the machine can be implemented. For the stator yoke, a boundary condition (i.e., Dirichlet) is imposed to the outer surface of the machine at $r = R_{out}$. Thus, there is no radial reluctance above the midpoint. The same condition is imposed on the rotor yoke at the inner surface at $r = R_{inner}$. Thus there is no radial reluctance below the midpoint. The tangential and radial reluctances used in the MEC are calculated by

$$\mathfrak{R}_r^i = \frac{1}{\mu_0 \cdot \mu_r^i \cdot L_{iron}} \cdot \frac{1}{\Theta^i} \cdot \ln \left(\frac{R_{out}^i}{R_{inner}^i} \right) \quad (3)$$

$$\mathfrak{R}_\theta^i = \frac{1}{\mu_0 \cdot \mu_r^i \cdot L_{iron}} \cdot \Theta^i \cdot \frac{1}{\ln \left(\frac{R_{out}^i}{R_{inner}^i} \right)} \quad (4)$$

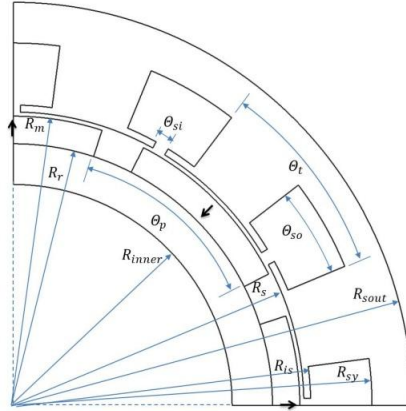


Figure 1. Cross section of 12-slots/8-poles CWPMMSM.

Table 1. Parameters of 12-slots/8-poles CWPMMSM

Parameters	Values
Number of phases, m [-]	3
Number of series turns per phase, N_{sts} [-]	28
Maximum current for a waveform sinusoidal, I_{smax} [A]	340
Rotation speed of the currents, N_0 [rpm]	3000
Mechanical angle of a pole-pitch, θ_p [deg.]	45
Mechanical angle of a tooth-pitch, θ_t [deg.]	30
Mechanical angle of a stator slot-isthmus, θ_{si} [deg.]	2.69
Mechanical angle of a stator slot-opening, θ_{so} [deg.]	14.87
Magnet pole-arc to pole-pitch ratio, α_p [%]	80
Stator slot-isthmus to tooth-pitch ratio, ζ_{si} [%]	8.97
Stator slot-opening to tooth-pitch ratio, ζ_{so} [%]	49.57
Relative magnetic permeability of iron (Linear), μ_{iron} [-]	3,000
Relative magnetic permeability of the PMs, μ_{rm} [-]	1.05
Remanent flux density of the PMs, B_{rm} [T]	1.3
Outer radius of the machine, R_{sout} [mm]	116.8
Radius of the stator yoke surface, R_{sy} [mm]	105
Radius of the stator isthmus, R_{is} [mm]	87

Radius of the stator surface, R_s [mm]	85
Radius of the PMs surface, R_m [mm]	83.8
Radius of the rotor yoke surface, R_r [mm]	75.8
Inner radius of the machine, R_{inner} [mm]	64
Machine axial length, L_{iron} [mm]	100

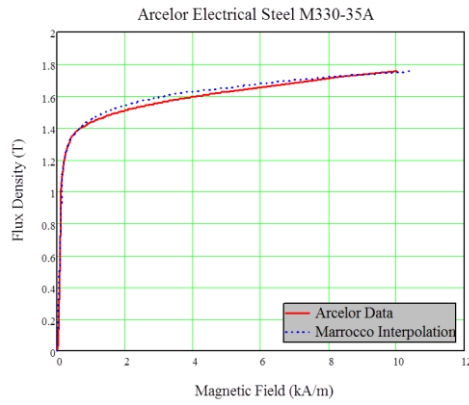
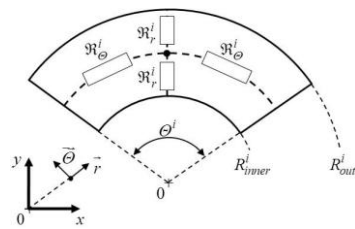
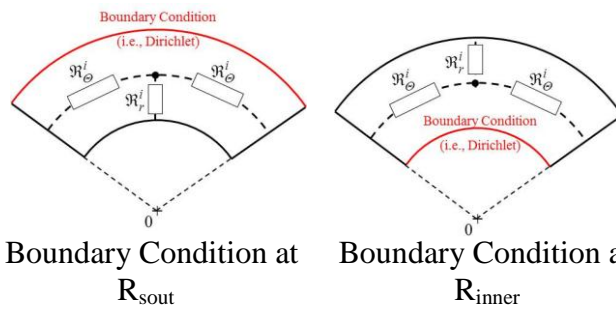


Figure 2. B(H) curves given by the manufacturer and Marrocco interpolation.



Reluctances for each region i



Boundary Condition at R_{sout}

Boundary Condition at R_{inner}

Figure 3. Reluctance for each region i of the machine and boundary conditions

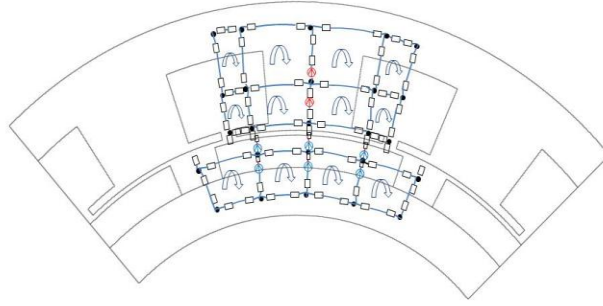


Figure 4. Discretization of the machine for one tooth-pitch and one pole-pitch.

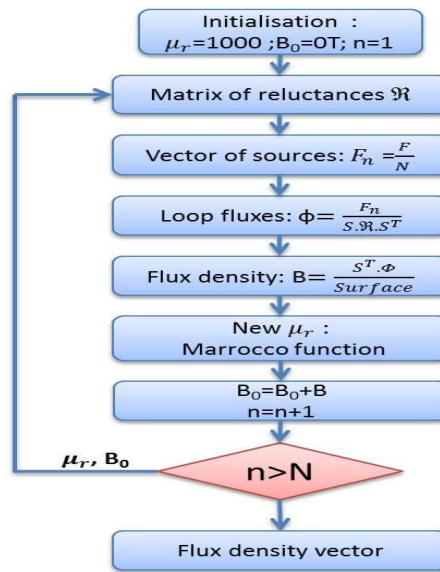


Figure 5. Different steps of the non-linear system resolution

2.4. MEC Modeling

The elementary discretization of the machine and the various reluctances considered in our study are presented in Figure 4. Only one tooth-pitch and one pole-pitch are considered.

To connect the loop fluxes and the reluctances, a loop matrix [S] is created. The connection between the sources vector [F], the reluctances matrix [R] and the loop fluxes vector [ψ] is defined by

$$[S] \cdot [R] \cdot [S]^T \cdot [\psi] - [F] = 0 \quad (5)$$

The connection between the loop fluxes vector [ψ] and the reluctance fluxes vector [ϕ] is described by [4]

$$[\phi] = [S]^T \cdot [\psi] \quad (6)$$

The sources vector [F], is composed by both the Magneto-Motive Force (MMF) due to the PMs and the MMF due to the current winding. The MMF provided by a PM is given by

$$MMF_{PM} = \frac{B_{rm}}{\mu_0 \cdot \mu_{rm}} \cdot h_m \quad (7)$$

while the MMF provided by one coil, containing n_t turns and fed by a current I_s , is expressed by

$$MMF_l = n_t \cdot I_s \quad (8)$$

The reluctances matrix $[\mathfrak{R}]$ is a diagonal matrix [NRXNR], where the diagonal is formed by the different reluctances. The loop fluxes matrix $[\psi]$ is a vector [NLX1] formed by the different loop fluxes. The sources matrix [F] has the same dimensions as the matrix $[\psi]$. The loop matrix [S] is constituted by NR columns and NL lines ([NLXNR]).

The non-linear system taking into account the saturation effect is solved iteratively. The vector [F] is divided into N parts (equal or not). Then, (5) and (6) are solved in order to obtain the reluctance fluxes vector $[\phi]$. Thus the reluctance flux density vector [B], is calculated using the vector $[\phi]$ and the reluctance surfaces vector [SR]. The new magnetic permeability can be calculated using (1) and (2), and the vector [B] is added to that obtained during the previous iteration. The different resolution steps are described in Figure 5.

The magnetic permeability is considered as constant in a range of a MMF equal to [F]/N for each iteration. Higher is the number of discretization N, higher the accuracy is.

3.1. Numerical Tool

The numerical tool used in this work to evaluate the efficiency and the performances of the MEC modeling approach is Flux 2D developed by Cedrat [10]. One pole pairs and three slots are considered for the simulation. A boundary condition is imposed to the inner and outer surface of the machine. The mesh considered is shown in Figure 6. The mesh is finer at the areas where variations of flux density are high (air gap and PMs) and larger elsewhere (stator yoke, rotor yoke, tooth and slot).

3.2. Precision based on the Magnetic Flux Density

In Figure (7) ~ (14) are presented the radial and tangential components of the no-load magnetic flux density in the different parts of the machine (i.e., the air-gap, the stator yoke, the PMs and the rotor yoke). The solid lines represent the magnetic flux density computed by FEA without saturation, the dashed lines shows the FEA results with saturation taken into account, and the circles corresponds to the magnetic flux density computed by MEC. One can see that there is a good agreement between the magnetic flux densities computed by FEA (with saturation effect) and those evaluated by the MEC. It proves the ability of the MEC to take into account the slotting effect and the magnetic saturation, even with a relatively small network.

3.3. Convergence and Computation Time

It must be noted that the resolution of the system of non-linear equation (5) and (6), can be done using Newton Raphson algorithm. The fact that the MEC is mesh based lead to a fast convergence and low number of iterations. In Table 2, we present the computation time for the MEC compared with the time needed to solve the problem using FEA. It is important to notice that we divide the computation time roughly by 10. This should enable easy implementation of the MEC with saturation in an optimization process for electric machines.

Table 2. Computation Time for the Different Method

	No Load	Load @ 240 Amax
FEA without saturation	56s	56s
FEA with saturation	190s	190s
MEC without saturation	5s	5s
MEC with saturation	20s	20s

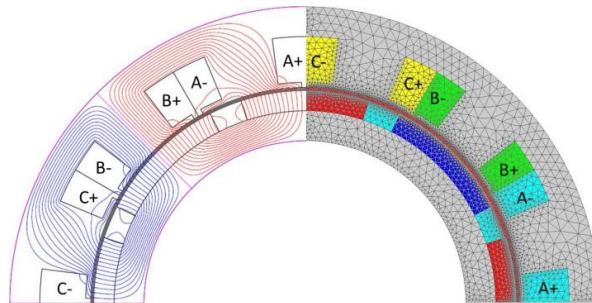


Figure 6. Mesh, winding configuration and magnetic field lines.

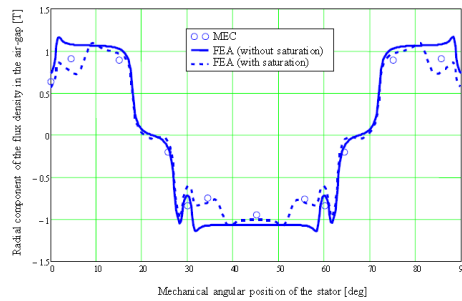


Figure 7. Radial component of the air-gap flux density.

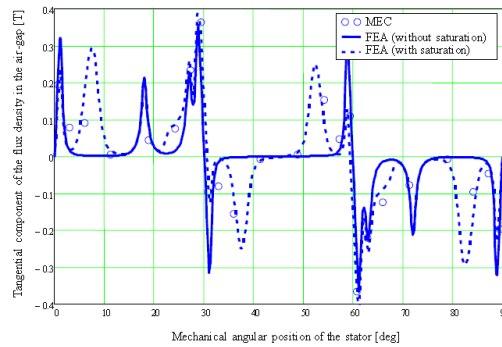


Figure 8. Tangential component of the air-gap flux density.

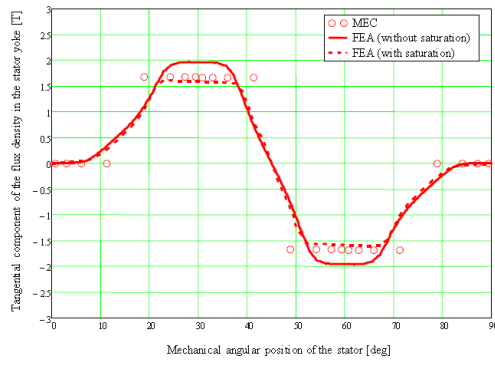


Figure 9. Tangential component of the stator yoke flux density.

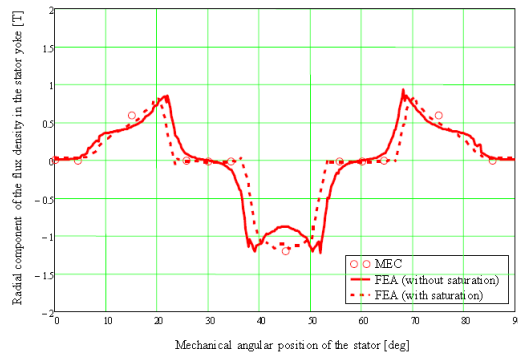


Figure 10. Radial component of the stator yoke flux density.

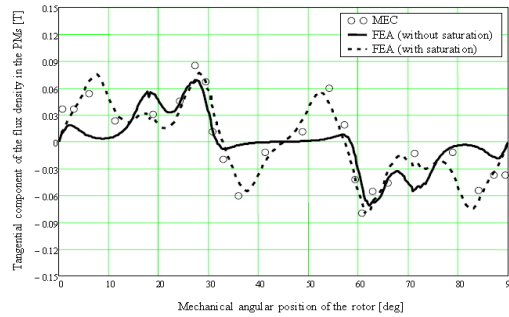


Figure 11. Tangential component of PMs flux density.

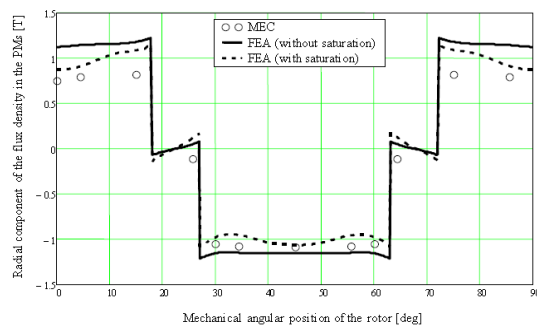


Figure 12. Radial component of PMs flux density.

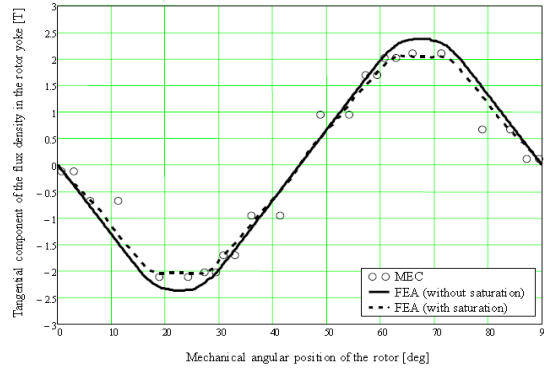


Figure 13. Tangential component of rotor yoke flux density.

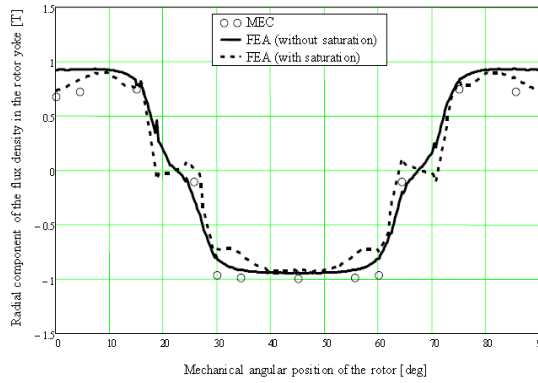


Figure 14. Radial component of rotor yoke flux density.

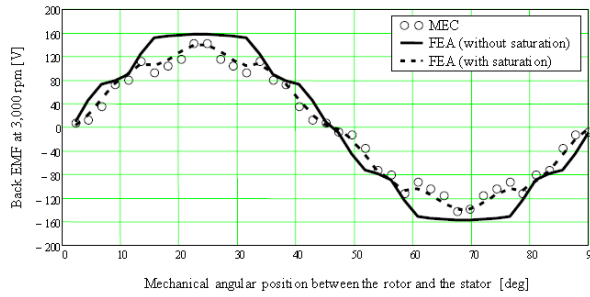


Figure 15. Phase Back EMF @ 3,000 rpm.

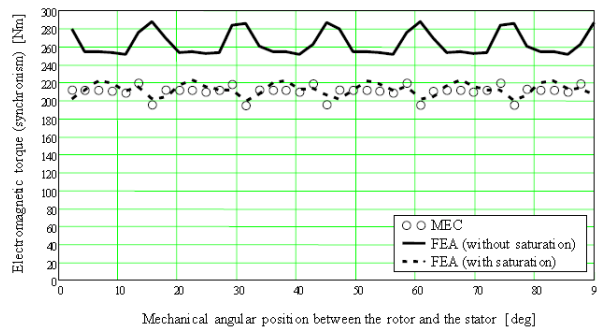


Figure 16. Electromagnetic torque computed @ 240 Amax.

4. Comparison Based on Integral Quantities – Back-EMF and Electromagnetic Torque

4.1. Back-EMF in phase-A

In Figure 15 we represent the Back-EMF in phase-A at 3,000 rpm computed by the three different methods: the solid line represents the Back-EMF computed by FEA assuming a linear characteristic of the iron, the dashed line corresponds to the FEA taken into account saturation, and circles represent the points obtained with the MEC. One can see that also for integral value of the machine, there is a good agreement between the results given by FEA and those calculated with MEC.

4.2. Electromagnetic Torque

The electromagnetic torque is an important output of our modeling. Indeed this value must be computed with a very good accuracy, since the torque produced by the drive should match with the technical specifications. In Figure 16 we depict three torque curves. The solid line shows the torque computed by FEA in linear condition, the dashed line shows the torque computed by FEA assuming the real B(H) characteristic and the circles corresponds to the points of torque computed by the MEC where the saturation effect is taken into account. It must be noted that the average torque when the saturation is taken into account is lower than the torque when we assume a linear iron steel. One can see also that the MEC modeling give us a quite satisfying correspondence in term of torque computation.

5. Conclusion

In this paper, we present a semi-analytical modeling approach suitable for the design of electric machine used in EV and HEV applications. The method presented is based on the MEC. The parametric modeling of a new electric machine may take time for the designer. Therefore once the model is built, the parametric study and machine optimization should be achieved easily. To illustrate the efficiency of the method, a 12-slots/8-poles concentrated winding PM synchronous machines is used as an example. The comparison between local quantities computed by FEA and those obtained by MEC shows a good agreement, and obviously the integral quantities (i.e., the back-EMF, the electromagnetic torque) correspond too. The main advantage of the MEC is that we can get a precision comparable to what we can obtain by FEA, and with computation time divide by 10. For this reason it should be easy to implement the MEC models in an optimization tool.

6. References

- [1] A. Marrocco, *"Analyse numérique de problèmes d'électrotechnique,"* Ann. Sc. Math. Québec, 1977, vol 1, No 2, pp 271-296
- [2] F. Hecht, A. Marrocco, F. Piriou, and A. Razek, *"Modélisation de systèmes électrotechniques par couplage des équations électriques et magnétiques,"* Rev. Phys. Appl. 1990, pp 649-659
- [3] F. Dubas, *"Conception d'un moteur rapide à aimants permanents pour l'entraînement de compresseurs de piles à combustibles,"* PhD Thesis, Université de Franche-Comté (France), December 2006
- [4] A. Delale, L. Albert, L. Gerbaud, and F. Wurtz, *"Automatic Generation of Sizing Models for the Optimization of Electromagnetic Devices Using Reluctance Networks,"* IEEE Trans. on Magn., vol. 40, no. 2, March 2004

- [5] S.A. Randi, "*Conception systématique de chaînes de traction synchrones pour véhicules électriques*," PhD Thesis, INP Toulouse (France), April 2003
- [6] V. Ostovic, "*A Simplified Approach to Magnetic Equivalent Circuit Modeling of Induction Machines*," *IEEE Trans. Ind. Appl.*, vol. 24, no. 2, pp. 308-316, March/April 1988
- [7] V. Ostovic, "*A Novel Method for Evaluation of Transient States in Saturated Electric Machines*," *IEEE Trans. Ind. Appl.*, vol. 25, no. 1, pp. 96-100, January/February 1989
- [8] C.B. Rasmussen, and E. Ritchie, "*Magnetic Equivalent Circuit Method For Designing Permanent Magnet Motors*," in *Proc. ICEM*, Vigo, Spain, Sept. 10-12, 1996
- [9] J.K. Tangudu, T.M. Jahns, A. EL-Refaie, "*Core Loss Prediction Using Magnetic Circuit Model for Fractional-Slot Concentrated-Winding Interior Permanent Magnet Machines*," Energy Conversion Congress and Exposition (ECCE), 2010
- [10] Flux2D, "*General operating instructions – Version 10.2.1.*", Cedrat S.A. Electrical Engineering, 2006, Grenoble, France

7. Glossary

HEV: Hybrid Electric Vehicle

EV: Electric Vehicle

CWPMMSM: Concentrated Winding Permanent Magnet Synchronous Machines

FEA: Finite Element Analysis

FEM: Finite Element Modelling

MEC: Magnetic Equivalent Circuit

PM: Permanent Magnet

MMF: Magneto-Motive Force

EMF: Electro-Motive Force